

# Direct manufacturing of thermoplastic parts by powder laser sintering: Comparison of coalescence simulations and Frenkel based physical model

D. Defauchy<sup>a,\*</sup>, G. Regnier<sup>a</sup>, P. Peyre<sup>a</sup>, I. Amran<sup>a</sup>, A. Ammar<sup>b</sup>

<sup>a</sup> Arts et Métiers ParisTech, PIMM, CNRS, Paris France.

<sup>b</sup> Arts et Métiers ParisTech, LAMPA, Angers France.

\*Corresponding author: [denis.defauchy@paris.ensam.fr](mailto:denis.defauchy@paris.ensam.fr)

**Abstract.** Direct manufacturing technology using Selective Laser Sintering (SLS) on polymer powders allows obtaining final parts in a short time, with a high degree of flexibility concerning shapes, evolution of parts and with classical polymer density. The physical base of this process is the coalescence of grains, which initiates the densification of powder during SLS. This study will present a comparison between a 2D C-NEM coalescence simulation and a 2D analytical model based on 3D Frenkel model in order to build a reference to simulate the process. Comparing our model to Frenkel's one, we firstly see that they are very close, and we observe that the 2D evolution is faster than the 3D one in the early stage of coalescence, but remains globally slower. The 2D process simulation enables us to validate the principles we will use in 3D.

## Introduction

Polymer Parts obtained by direct manufacturing with laser sintering technology present porosities [1] which significantly reduce their mechanical resistance [2]. Then, it is important to be able to predict the conditions in which porosity volume will be minimal. This porosity is due to the air between polymer powder grains which remains trapped in the material while polymer is melting. As the process needs to be performed with temperature variations, air volume evolutions have to be taken into account, influencing directly the density of the material.

**The process.** The important material parameters acting in the process which appear globally in the whole literature concern viscosity of the polymer, surface tension, density, heat capacity, grains size and dispersion, thermal conductivity and laser absorptivity.

Parts manufacturing by SLS is difficult for some reasons. Firstly, the polymer powder degrades while performed in the machines [3] maintained at high temperatures for some hours. It is also difficult to predict the polymer solidification, which depends on the cooling conditions as semicrystalline polymers are mainly used [4]. Furthermore, there

are multiple parameters which influence the final material.

Among all articles cited here, it appears that the main controllable process parameters influencing the final material can be classed in order of importance [5]: layer thickness, laser speed, pre-heating powder bed temperature and laser power (most important). Some of these results have been confirmed through a finite element model [6]. Some other parameters are discussed as laser beam diameter, hatch distance and layering conditions. It seems clear that the use of a CO<sub>2</sub> laser (10.6 μm) to melt the polymer powder is recommended.

All these parameters are often connected. For example, when particle size is decreased, the layering becomes difficult [4]. Among all articles cited here, studies concerning the influence of each process parameters and their relation on the final material can be found.

Some experiments have been done to obtain better performances in parts manufacturing, using multiple laser sources working on the same layer [7,8], or using a variable laser beam diameter [9].

In terms of results of the process on parts, the different studies available in the literature are

concerning density, mechanical resistance [2,10], building time, surface state [11] and geometrical defects [11].

A recent study [12] models the mechanical behavior of SLS parts, considering holes in a bulk material in order to represent porosities, and compares the model with experimental parts of the same density. However, the results were not in good agreement with experiments.

To conclude on the process, all this work in the last ten years has been made to find the best parameters to manufacture parts with good density and mechanical performances. A lot of parameters influence the quality of parts obtained by SLS, and still today, it seems important to continue to try to find the best conditions to become more competitive and efficient. Nevertheless, the best process conditions are usually found by making a lot of tests to choose the best parameters for each material.

**Simulation needs.** In parallel to the experiences, it is important to simulate the process for a better understanding of the parts characteristics. Simulating the process will enable to choose the best parameters for the manufacturing and predict the performances of SLS polymer parts, and as soon as the simulation is functional, have this information faster.

In order to simulate the process, understanding its physical base is necessary. Under the action of the laser, the powder is densified. This densification is due to the coalescence of particles, which is driven by surface tension, while viscosity, geometry, gravity and temperature change the kinetics of the process. Coalescence models are also needed to validate the simulations.

**Coalescence analytical modeling.** The evolution of the coalescence of two liquid spheres can be described by analytic models. The first model found in the literature is Frenkel's model [13]. Supposing a spherical shape for the system composed by two particles and the only contribution of surface tension as motor of the phenomena and the fluid viscosity as dissipation, it is possible to obtain a simple evolution of the dimensionless neck radius at the early stage of

coalescence. Eshelby [14] proposed a modification of the model to take into account the fluid incompressibility. Later, Pokluda et al. [15,16] computed the resolution of Frenkel's model considering the evolution of the radius from both particles, and presented results compared with experiments, which represented quite well the observations.

However, we can take some precautions regarding the problems we can observe in heat chamber under microscope because of the surface tension on support between air, polymer and support, which is able to considerably change the kinetics of coalescence and shape of the particles.

**Objectives.** Our objective is to simulate the SLS process in order to predict part's density. We also have to begin with a 2D model (infinite cylinders) in order to simplify the development and validate the principles, using experiments performed on polymer fibers. We will then present a 2D simulation of the process before trying to compute the simulation in 3D.

We will first present our 2D Frenkel based model and compare it to the 3D model. We will then expose our C-NEM simulation performed on Matlab and compare the simulation to the model results. Finally, we will expose the 2D process simulation performed on multi-cylinders before discussing future work.

## Development of a Frenkel based 2D model

In order to be able to have a comparison with physics, we developed a 2D Frenkel model, corresponding to the coalescence of infinite cylinders.

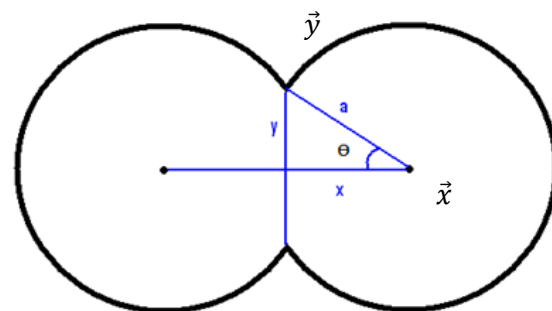


**Fig. 1.** Shape of two cylinders during coalescence - Definition of parameters.

We are placed in the same assumptions that Frenkel, Eshelby and Pokluda, considering that both of the particles stay circular (Fig. 1.), and we suggest the 2D deformation tensor  $D$  as follows:

$$D = \begin{bmatrix} -\dot{\epsilon} & 0 \\ 0 & \dot{\epsilon} \end{bmatrix} \quad (1)$$

We are then able to calculate the power developed by surface tension  $P_{st}$ :

$$P_{st} = -\Gamma \frac{d}{dt} [4(\pi - \theta)a(t)] \quad (2)$$

The power dissipated by viscosity  $P_{visc}$  is:

$$P_{visc} = \int_S 4\eta \dot{\epsilon}^2 dS = 8\pi a_0^2 \eta \dot{\epsilon}^2 \quad (3)$$

Equalizing the two power acting in the phenomenon, we finally obtain the differential equation giving  $\theta$  evolution with time:

$$\frac{d\theta}{dt} = \frac{\Gamma}{\eta a_0} \frac{1}{2\sqrt{\pi}} \left[ \frac{(\cos\theta + \frac{\sin\theta}{\pi-\theta}) \cos\theta (\pi - \theta + \frac{\sin 2\theta}{2})^{\frac{1}{2}}}{\sin\theta^2 (\pi-\theta)} \right] \quad (4)$$

to be compared to the 3D one:

$$\frac{d\theta}{dt} = \frac{\Gamma}{\eta a_0} 2^{\frac{-5}{3}} \left[ \frac{\cos\theta (1 + \cos\theta)^{\frac{2}{3}} (2 - \cos\theta)^{\frac{1}{3}}}{\sin\theta} \right] \quad (5)$$

We can define the dimensionless time  $\tau$  as follows:

$$\tau = \frac{t\Gamma}{\eta a_0} \quad (6)$$

We can finally present our simplified coalescence model for infinite cylinders:

$$\frac{y}{a} = \sin \left( \left( \frac{3}{2\pi} \tau \right)^{\frac{1}{3}} \right) \quad (7)$$

This model is compared to a modified 3D Frenkel's one, adding the sine to the model, because it seems to better correspond to the true coalescence evolution:

$$\frac{y}{a} = \sin \left( \tau^{\frac{1}{2}} \right) \quad (8)$$

This solution is not overpassing the value of 1, and seems to represent the phenomenon after the early stage of coalescence (Fig. 2.). We can indeed calculate the real solution of the differential equation by increments with a Taylor development, and compare, not only for our 2D Frenkel based model but also for the 3D Frenkel's model, and see that the simplified solution approximated on zero is very close to the solution of the differential equation of the whole phenomenon, which result was not that expectable.

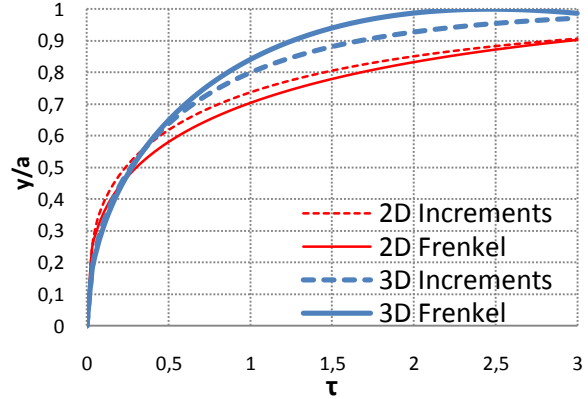


**Fig. 2.** Comparison between 2D and 3D Frenkel model.

We can firstly see that both 2D and 3D models are quite similar. We can furthermore observe that the 2D phenomenon is faster than the 3D one in the early stage of the coalescence, but the 3D model is rapidly faster than the 2D one.

### Development of C-NEM simulation

The C-NEM method (Constrained Natural Element Method) [17,18] is very interesting because of its meshless character, which is free of mesh problems, as a fluid is moving and the nodes can take some bad positions regarding classical finite element methods. Using C-NEM method also exempts volume remeshing.

**Coalescence simulation.** We performed a C-NEM numerical simulation of polymer infinite cylinders coalescence (2D) to be able to validate the calculation. The simulation, implemented in Matlab, considers an isothermal viscous incompressible fluid including surface tension, without any contact with support, pressure and gravity. As flows are very slow, due to high

viscosities, inertial terms are neglected. We resolve a mixed formulation in velocity and pressure, so that we have 3 degrees of freedom per node. In parallel, we calculate the temperature of each node with the same C-NEM method. We put an initial neck radius for calculation consideration. Particular work is made to discretize as well as possible the interface between air and polymer. Mesh is indeed adapted to the local curvature of the interface through a local remeshing. We add displacement conditions to block rigid body movements with Lagrangian conditions on all nodes, in order not to concentrate defects on only one node. There are indeed some calculations problems, as the system is geometrically discretized, and the resultant global surface tension is not zero. If we just block one node for x and y displacement, and as we compute fluids, the shape of the system is extremely affected by this condition.

Concerning numerical simulation, the velocity (UV) is interpolated by constrained Sibson natural element shape functions while the pressure P is assumed as constant by cell. The weak formulation integration is done by nodal integration. For velocity gradient we use the SCNI method (Stabilized Conform Modal Integration).

The physical parameters as surface tension, surface power flux, volume power flux and gravity are assumed as piecewise constants.

We are now able to simulate the coalescence of two infinite cylinders to compare with the analytical model.

**Process simulation.** We only worked in 2D at this time. We performed a simulation on 12 cylinders lying on a support in the studied area (Fig. 3.).

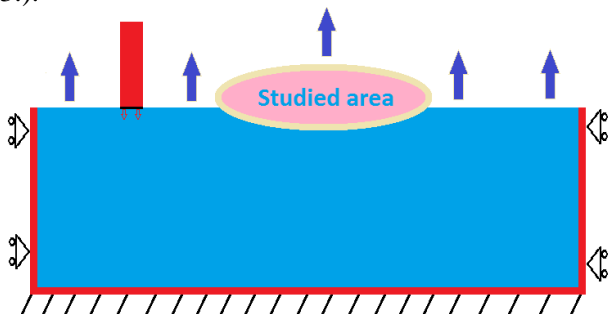


**Fig. 3.** Thermal and displacement limit conditions of the simulation

Considering the previous simulation, we added thermal conditions, new displacement conditions and air consideration, in order to take into account the density.

The thermal conditions (Fig. 3.) that we impose at the beginning are the initial temperature of the polymer in the whole domain, a temperature on the 3 borders (solid line on Fig. 3.) staying constant during all the simulation, a convection exchange on the free surface on the top of the domain (arrows on Fig. 3.) with a chosen constant air temperature, and we suppose that the air in cavities is not conductive. A laser is scanned during the simulation from the left to the right with a chosen velocity and applies the power very rapidly (some ms) using a model found in the literature [19], considering only a surface heat flux. The air in the cavities is supposed to obey the ideal gas law. We however do not impose the pressure on the borders, as we had to simulate the movements with an extremely small time step because of the small volumes of the cavities. A small variation of volume induces a big variation of pressure, and we could observe oscillations of the volumes of the cavities around the equilibrium state. These variations were observed even with small time step, which is not so useful for a heavy calculation. We chose to impose the volume of the cavities, deduced from the ideal gas law, through a Lagrangian method on the velocity of the nodes. We were then able to impose the derivative of the volume, coupled with the time step to obtain the desired volume at each time step. The only parameter depending on the temperature at this time is the viscosity, following an Arrhenius law as follows:

$$\mu(T) = Ke^{\frac{E}{RT}} \quad (9)$$

The thermal dependence of the heat capacity  $C_p$  and the surface tension  $\Gamma$  can be performed.

The system is supposed to be blocked on the bottom, (Fig. 3.) and we impose symmetry conditions on the borders (left and right) for the velocity. The domain has to be large enough not to influence the melting area.

We can then make post treatments on the system, getting the evolution of cavities volumes and the density of the final part.

## Results and discussions

**Comparison of simulation with analytical model.** It seems to be difficult to compare the same things, considering the variables  $y$  and  $a$  to calculate the dimensionless neck radius, because in reality, the shape is not standing as perfect as supposed in the model (Fig. 1.).

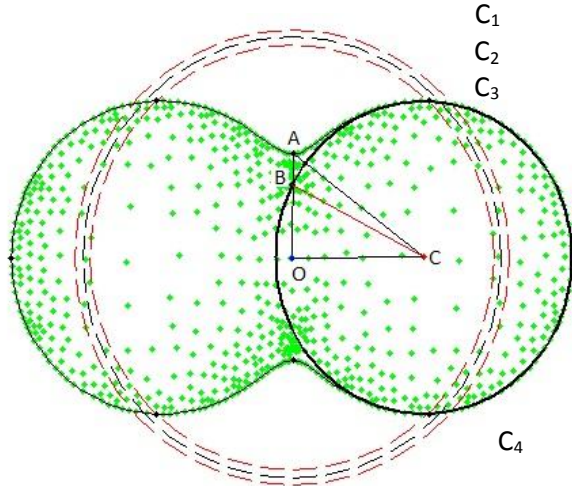


**Fig. 4.** Capture during the coalescence simulation - Definition of simulated parameters.

We can see on the capture (Fig. 4.) the nodes of the domain and 4 points A, B, C and D, which represent particular area where we can measure coalescence parameters versus time, and the final position by the central dashed circle  $C_2$  among the three ones, the two surrounding dashed lines  $C_1$  &  $C_3$  representing the criteria to stop the simulation. The right circle  $C_4$  of radius  $CB$  represents a least square circle approximated on the right half circle of the right particle. We also choose different parameters to represent the simulation (Eq. 10.).

$$\begin{cases} y_{med} = OB \\ a_{med} = CB \\ y_{max} = OA \\ a_{max} = CA \end{cases} \quad (10)$$

We studied three different ratios (eq. 11) to try to approach Frenkel's representation. The first ratio (eq. 11. a) appears to represent quite well our model, as we take the apparent dimensionless neck radius, and the best volume we can imagine comparing to the model. The two other ratios (eq. 11. b & c) seem to be two other solutions which appear to encompass the model solution.

$$\begin{cases} [a] \frac{y_{max}}{a_{med}} \\ [b] \frac{y_{max}}{a_{max}} \\ [c] \frac{y_{med}}{a_{med}} \end{cases} \quad (11)$$

The results of the comparison between our analytic model based on Frenkel's model and the simulation are presented (Fig. 5.). We however did not find what we expected.

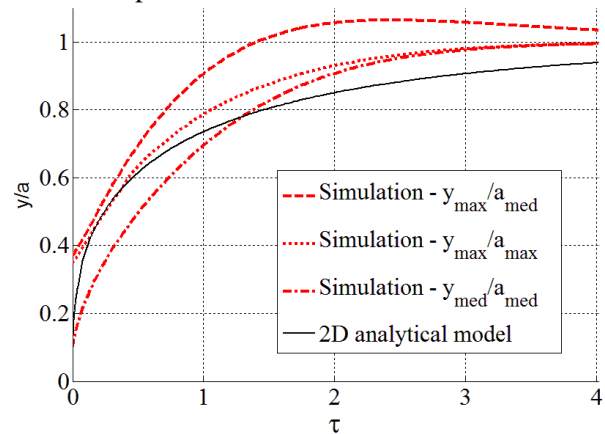


**Fig. 5.** Comparison between our 2D model and simulation.

**Table 1.** Process simulation parameters

Process parameters	Value	Material parameters	Value
Initial polymer temperature	150 °C	Cylinders diameter	100 μm
Boarder temperature	350 °C	Polymer Thermal conductivity	0.25 W.m <sup>-1</sup> .K <sup>-1</sup>
Air temperature	150 °C	Polymer density	1100 Kg.m <sup>-3</sup>
Exchange convection coefficient	13 W.m <sup>-1</sup> .k <sup>-1</sup>	Air density	1.2 Kg.m <sup>-3</sup>
Laser power	5.10 <sup>-7</sup> W	Gravity	9.81 m.s <sup>-2</sup>
Laser beam diameter	200 μm	Surface Tension	0.03 N.m <sup>-1</sup>
Laser velocity	1 m.s <sup>-1</sup>	Polymer heat capacity	1700 J.Kg <sup>-1</sup> .K <sup>-1</sup>
Laser reflectivity	4 %	Arrhenius K (PA 12)	3.5*10-6
		Arrhenius E (PA 12)	75647

Comparing the theoretical curve with the simulated coalescence, we can see that the simulation, even if we look at ratio a, b or c, is slower in the early stage of coalescence and globally faster than the analytic one.

Concerning the hypothesis of the shape of the system (two perfect cylinders), as we said, we could have expected that the curve representing medium values would have minimized the theoretical curve while the maximum values would have maximized it. It is however not the case.

We can imagine that the hypothesis of a constant circular shape is not the origin of these inappropriate results. We expect that the strong hypothesis which changes the results is the deformation tensor  $D$  (eq. 1.).

Experiments should help us to confirm this assumption.

**Process simulations.** We simulated the coarsening of twelve polymer fibers lying on a support of the same material. Table 1 presents the material and process parameters used in the simulation. We can see three captures of the process 2D simulation (Fig.6 a, b & c). As we are in 2D conditions, the air is not able to go out from the cavities. At the beginning (Fig. 6. a), the material is preheated, and we continue to impose a higher temperature on the border on the domain to induce the densification, and the laser passes after 5 seconds (Fig.6 b). The simulation time is about 10 seconds (Fig. 6. c). Normally, during the SLS process, only the laser causes the melting of the powder, but in order to validate the principle, we make the melting with the borders heating conditions added to the laser heating.

Our first results show that the laser model considering only a surface heat flux in the laser beam area is false (very high temperatures in order of  $15000^{\circ}\text{C}$  obtained, results confirmed with COMSOL simulation) and we will have to modify this model to impose a volume heat flux according to Beer-Lambert's law. Indeed, the simulation presented here has been adapted to lower the temperatures, with a laser power of  $5.10^{-7}$  W instead of 5 W. We can also understand that the laser doesn't induce a huge change in the melting phase.

We could however see an increase of temperature under laser irradiation of about  $1500^{\circ}\text{C}$  during some ms, until energy was dissipated by convection exchanges with the air.

These problems of high temperatures on some nodes induce numerical problems, conducting to very small time steps and indeed large calculation times. We can also realize that there are some internal fluid pressure problems on the borders. We will maybe have to impose this internal fluid pressure at the surface tension value to correct some problems.

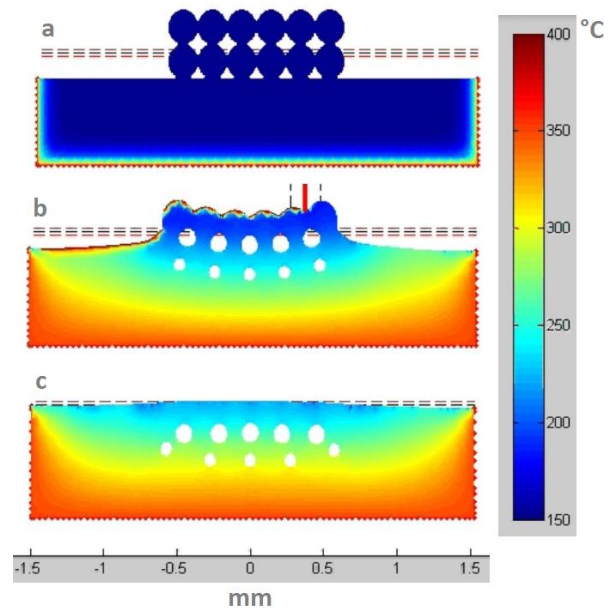


**Fig. 6.** Captures of simulation evolution (a - solid polymer, b - laser pass, c - melted polymer) during the SLS process applied on 12 cylinders.

Our resolution is considering a degree of freedom vector with velocities (order of  $10^{-6}$  m.s $^{-1}$ ) and relative pressure (order of  $10^2$  Pa), and we are confronted to numerical problems trying to resolve the calculation with iterative methods (Gmres function in Matlab). The next step will be to resolve the equations, decoupling velocity and pressure in order to make the iterative calculation possible, and thus not use too much RAM memory in computers.

Finally, we encounter some border problems, coming from the description of the surface tension calculated on each node by three points and a circle. We assume that it is linked with the problems we described before, and will use some curve fitting and relaxation methods to limit this phenomenon if

necessary. Furthermore, we will integrate a second degree of integration in the border terms (mainly for surface tension), which will converge to a better solution to reduce these problems.

### Conclusion and Perspectives

We made a 2D coalescence model and compared it with Frenkel's 3D one. We performed a numerical simulation which has been validated with our 2D model for two infinite polymer cylinders. The results show some differences, maybe due to hypothesis on the analytical model. In the next future, we plan to validate our results with experiments performed on polymer fibers in heat chamber under microscope in order to study a "2D" coalescence of infinite cylinders. We are now able to simulate the process in 2D on twelve cylinders, taking into account the complex multi-physical problem. After some improvement in parameters depending on temperature, laser modeling, and maybe taking into account an air diffusion model through the polymer [20], and some changes to avoid some numeric problems, we expect to upgrade the simulation in 3D to simulate the whole process, taking into account the possibility to the air to go through the holes out of the material, which is not physically in 2D.

### Acknowledgments

This study takes place in the FUI Project FADIPLAST. We thank Francisco Chinesta as he participated and supported this study.

### References

1. G.V. Salmoria, J.L. Leite, R.A. Paggi, *Polymer Testing*, **28**, 746 (2009).
2. M. Schmidt, D. Pohle, T. Rechtenwald, *CIRP Annals - Manufacturing Technology*, **56**, 205 (2007).
3. D.T. Pham, K.D. Dotchev, W.A.Y. Yusoff, *Proceedings of the Institution of Mechanical Engineers, Part C: Journal of Mechanical Engineering Science*, **222**, 2163 (2008).
4. V.E. Beal, R.A. Paggi, G.V. Salmoria, A. Lago, *Journal of Applied Polymer Science*, **113**, 2910 (2009).
5. P. Wang, X. Li, J. Xiao, F. Zhu, Y. Yang, *ICALEO 2006 - 25th International Congress on Applications of Laser and Electro-Optics, Congress Proceedings*, art. 517 (2006).
6. L. Dong, A. Makradi, S. Ahzi, Y. Remond, *Journal of Materials Processing Technology*, **209**, 700 (2009).
7. D.S. Kim, Y.J. An, K.H. Choi, *24th International Congress on Applications of Lasers and Electro-Optics, ICALEO 2005 - Congress Proceedings*, 296 (2005).
8. D.S. Kim, Y.J. Ahn, S.W. Bae, B.O. Choi, K.H. Choi, *ICALEO 2006*, 905 (2006).
9. S.W. Bae, D.S. Kim, K.H. Choi, S.Y. Yoo, *ICALEO 2008 - 27th International Congress on Applications of Lasers and Electro-Optics, Congress Proceedings*, 49 (2008).
10. H.C.H. Ho, I. Gibson, W.L. Cheung, *Journal of Materials Processing Technology*, **89-90**, 204 (1999).
11. J.-P. Kruth, G. Levy, F. Klocke, T.H.C. Childs, *CIRP Annals - Manufacturing Technology*, **56**, 730 (2007).
12. U. Ajoku, N. Hopkinson, M. Caine, *Materials Science and Engineering A*, **428**, 211 (2006).
13. J. Frenkel, *J. PhysNature*, **9**, 385 (1945).
14. J.D. Eshelby, *Metallurgical Transactions*, **185**, 796 (1949).
15. O. Pokluda, C.T. Bellehumeur, J. Vlachopoulos, *AIChE Journal*, **43**, 3253 (1997).
16. C.T Bellehumeur, M. Kontopoulou, J. Vlachopoulos, *Rheologica Acta*, **37**, 270 (1998).
17. J. Yvonnet, D. Ryckelynck, P. Lorong, F. Chinesta, *International Journal for Numerical Methods in Engineering*, **60**, 1451 (2004).
18. I. Alfaro, J. Yvonnet, F. Chinesta, E. Cueto, *International Journal for Numerical Methods in Engineering*, **71**, 1436 (2007).
19. L. Dong, A. Makradi, S. Ahzi, Y. Remond, *Journal of Materials Processing Technology*, **209**, 700 (2009).
20. G. Gogos, *Polymer Engineering and Science*, **44**, 388 (2004).